Inorg. Chem. **2009**, *48*, 2993−2999

Aqueous Fluorometric and Colorimetric Sensing of Phosphate Ions by a Fluorescent Dinuclear Zinc Complex

Snehadrinarayan Khatua, Shin Hei Choi, Junseong Lee, Kibong Kim, Youngkyu Do, and David G. Churchill*

Molecular Logic Gate Laboratory, Department of Chemistry, Korea Advanced Institute of Science and Technology (KAIST), 373-1 Guseong-dong, Yuseong-gu, Daejeon 305-701, Republic of Korea

Received November 21, 2008

A fluorescent dinuclear zinc complex (**1**) has been prepared by an easy "one pot" method in which the lysine-based Schiff base ligand is generated in situ. The compound is characterized in detail by various spectroscopic techniques and single-crystal X-ray diffraction. Crystal data: monoclinic, *C*2, $a = 18.31(13)$ Å, $b = 8.45(7)$ Å, $c = 11.20(8)$ Å, $\beta = 90.11(6)°$, $V = 1733.6(2)$ Å^3. $Z = 2$, *R1* = 0.0442, *wR2* = 0.1068, Flack(x) parameter = 0.03(2). Compound **1** is highly fluorescent, in both the solution phase and as a solid. Under neutral aqueous conditions (0.01 M HEPES buffer, pH 7.4), compound **1** exhibits intense blue fluorescence ($\lambda_{ex} = 352$ nm, $\lambda_{em} = 453$ nm, $\Phi_F = 0.17$). The complex was tested with several anions, such as F^-, Br^-, I^-, AcO^-, HCO_3^-, $H_2PO_4^-$, HPO_4^{2-}, PO_4^{3-}, and a variety of biologically relevant phosphate anions, such as adenosine monophosphate (AMP), cyclic adenosine monophosphate (cAMP), inorganic pyrophosphate (PPi, $P_2O_7^{4-}$), adenosine diphosphate (ADP), and adenosine triphosphate (ATP), in water at physiological pH. The dizinc species was found to act as a highly selective sensor for PPi in particular by fluorescence ON-OFF signaling. Both the fluorometric and colorimetric (indicator displacement assays) titration results suggest that compound **1** is a highly selective sensor for phosphate ions with the order PPi ≥ ATP > ADP.

Introduction

Anions play a vital role in chemistry and biology. The design and synthesis of anion-selective receptors or sensors have received considerable attention.[1] In particular, fluorescent anion sensors are very appealing because they allow for low detection limit analysis.[2] The development of selective receptors for phosphate anions and derivatives, such as HPO_4^{2-}, pyrophosphate (PPi, $P_2O_7^{4-}$), adenosine triphosphate (ATP), adenosine diphosphate (ADP), CTP_3, IP_3, and phosphoproteins, has been of particular interest because of the vital roles that these chemical species play in a range of life processes. These processes involve such essential events as energy storage, signal transduction, and gene construction.[3] Especially, PPi is a biologically important target because it is the product of ATP hydrolysis under cellular conditions.[4]

* To whom correspondence should be addressed. E-mail: dchurchill@kaist.ac.kr.

(1) For reviews of these topics, please regard: (a) Lipscomb, W. N.; Sträter, N. *Chem. Rev.* **1996**, *96*, 2375. (b) Gale, P. A. *Acc. Chem. Res.* **2006**, *39*, 465. (c) O'Neil, E. J.; Smith, B. D. *Coord. Chem. Rev.* **2006**, *250*, 3068. (d) Beer, P. D.; Gale, P. A. *Angew. Chem., Int. Ed.* **2001**, *40*, 486. (e) Yoon, J.; Kim, S. K.; Singh, N. J.; Kim, K. S. *Chem. Soc. Rev.* **2006**, *35*, 355.

(2) (a) de Silva, A. P.; Gunaratne, H. Q. N.; Gunnlaugsson, T.; Huxley, A. J. M.; McCoy, C. P.; Rademacher, J. T.; Rice, T. E. *Chem. Rev.* **1997**, *97*, 1515. (b) Schmidtchen, F. P.; Berger, M. *Chem. Rev.* **1997**, *97*, 1609. (c) Lee, H. N.; Swamy, K. M. K.; Kim, S. K.; Kwon, J.-Y.; Kim, Y.; Kim, S.-J.; Yoon, Y. J.; Yoon, J. *Org. Lett.* **2007**, *9*, 243, and references therein.

(3) For HPO_4^{2-} sensing, see: (a) Han, M. S.; Kim, D. H. *Angew. Chem., Int. Ed.* **2002**, *41*, 3809; for PPi sensing, see: (b) Jang, Y. J.; Jun, E. J.; Lee, Y. J.; Kim, Y. S.; Kim, J. S.; Yoon, J. *J. Org. Chem.* **2005**, *70*, 9603. (c) Fabbrizzi, L.; Marcotte, N.; Stomeo, F.; Taglietti, A. *Angew. Chem., Int. Ed.* **2002**, *41*, 3811; for ATP sensing, see: (d) Ojida, A.; Nonaka, H.; Miyahara, Y.; Tamaru, S.-I.; Sada, K.; Hamachi, I. *Angew. Chem., Int. Ed.* **2006**, *45*, 5518; for CTP_3 sensing, see: (e) Nikura, K.; Anslyn, E. V. *J. Am. Chem. Soc.* **1998**, *120*, 8533; for IP_3 sensing, see: (f) Oh, D. J.; Ahn, K. H. *Org. Lett.* **2008**, *10*, 3539; for phosphoprotein sensing, see: (g) Aoki, S.; Zulkefeli, M.; Shiro, M.; Kohsako, M.; Takeda, K.; Kimura, E. *J. Am. Chem. Soc.* **2005**, *127*, 9129. (h) Anai, T.; Nakata, E.; Koshi, Y.; Ojida, A.; Hamachi, I. *J. Am. Chem. Soc.* **2007**, *129*, 6232; PPi polymer sensing, see: (i) Aldakov, D.; Anzenbacher, P., Jr. *J. Am. Chem. Soc.* **2004**, *126*, 4752; for recent articles on PPi and ATP sensing, see: (j) Huang, X.; Guo, Z.; Zhu, W.; Xie, Y.; Tian, H. *Chem.Commun.* **2008**, 5143. (k) Ojida, A.; Takashima, I.; Kohira, T.; Nonaka, H.; Hamachi, I. *J. Am. Chem. Soc.* **2008**, *130*, 12095.

(4) (a) Mathews, C. P.; van Holde, K. E.; *Biochemistry*; Benjamin/Cummings Publishing Company, Inc.: Redwood City, CA, 1990. (b) Nyrén, P. *Anal. Biochem.* **1987**, *167*, 235. (c) Tabary, T.; Ju, L. *J. Immunol. Methods.* **1992**, *156*, 55.

10.1021/ic8022387 CCC: $40.75
Published on Web 03/05/2009

Table 1. Crystal Data for Complex **1**

empirical formula	$C_{28}H_{48}Cl_2N_4O_{11}Zn_2$
formula weight	818.34
temperature, wavelength	296(2) K, 0.71073 Å
crystal system, space group	monoclinic, *C*2
unit cell dimensions	a = 18.3133(13) Å b = 8.4505(7) Å β= 90.115(6)° c = 11.2021(8) Å
volume	1733.6(2) Å^3
Z	2
density (calculated)	1.568 Mg/m^3
absorption coefficient	1.599 mm^{-1}
F(000)	852
crystal size	0.20 × 0.10 × 0.10 mm^3
theta range for data collection	1.82 to 28.32°.
reflections collected	7798
independent reflections	3343 [*R*(int) = 0.0412]
completeness to theta = 28.32°	97.6%
absorption correction	empirical
max. and min. transmission	0.88 and 0.79
refinement method	full-matrix least-squares on F^2
data/restraints/parameters	3343/5/195
goodness-of-fit on F^2	1.055
final *R* indices [$I > 2$sigma(I)][a]	R1 = 0.0442, wR2 = 0.1068
R indices (all data)[a]	R1 = 0.0699, wR2 = 0.1282
absolute structure parameter	0.03(2)

[a] $R1 = \sum||F_o| - |F_c||/\sum|F_o|$; $wR2 = \{\sum[w(F_o^2 - F_c^2)^2]/\sum w(F_o^2)^2\}^{1/2}$.

Table 2. Selected Bond Lengths [Å] and Angles [deg] for Compound **1** around the Zn(1) Center[a]

Bond Lengths			
Zn(1)−N(1)	2.0687(19)	O(1)−Zn(1)#1	2.0345(18)
Zn(1)−O(1)	2.0753(19)	Zn(1)−O(2)	2.0902(19)
Zn(1)−O(1)#1	2.0345(16)	Zn(1)−Cl(1)	2.2815(18)
Bond Angles			
C(7)−N(1)−Zn(1)	128.6(3)	C(8)−N(1)−Zn(1)	111.9(2)
C(1)−O(1)−Zn(1)#1	127.3(2)	C(1)−O(1)−Zn(1)	129.0(2)
Zn(1)#1−O(1)−Zn(1)	102.32(9)	C(9)−O(2)−Zn(1)	115.4(3)
O(1)#1−Zn(1)−N(1)	145.95(10)	O(1)#1−Zn(1)−O(1)	77.62(9)
N(1)−Zn(1)−O(1)	86.45(9)	O(1)#1−Zn(1)−O(2)	94.68(7)
N(1)−Zn(1)−O(2)	78.79(7)	O(1)−Zn(1)−O(2)	140.61(11)
N(1)−Zn(1)−Cl(1)	109.53(7)	O(1)−Zn(1)−Cl(1)	108.43(8)
O(2)−Zn(1)−Cl(1)	110.90(8)	O(1)#1−Zn(1)−Cl(1)	104.04(7)

[a] Note: Symmetry transformations used to generate equivalent atoms: #1: $-x + 1$, y, $-z + 1$.

Similarly, ATP is also a very important sensing target because it is known as a universal energy source and is also involved in many enzymatic reactions inside living organisms.[4] While a variety of fluorescent PPi-selective sensors have been reported, only a few involve both fluorometric and colorimetric methods that are able to conveniently be used in a pure aqueous medium.[3d,5] Though a large number of reported phosphate sensors involve Zn^{2+} and a 2,2′-dipicolylamine arm, there are no reports, to the best of our knowledge, of Zn^{2+}-based phosphate sensing complexes derived from a natural amino acid in which this portion becomes part of the metal ligating motif.[2c,3a,b,d,g,5,6]

Herein, we report the synthesis of a dinuclear chiral complex, $[Zn_2(slys)_2Cl_2]\cdot(CH_3OH)_2\cdot(H_2O)_3$ {hereafter, **1**·$(CH_3OH)_2$·$(H_2O)_3$} [H_2slys = 6-amino-2-{(2-hydroxybenzylidene)amino} hexanoic acid] from an in situ formed L-lysine-based ligand. The compound was characterized in detail by various spectroscopic techniques as well as by single-crystal X-ray diffraction. Since this species is both fluorescent and extremely water soluble, we can conduct aqueous fluorimetric and colorimetric sensing of biologically important PPi and of the closely related species ATP and ADP under physiological pH.

Experimental Section

Materials and Physical Measurements. All chemicals herein were used as received from commercial suppliers (Aldrich and TCI companies). ^{1}H and ^{13}C NMR spectra were measured on a Bruker Avance 400 MHz spectrometer using TMS as the internal standard. Spectral signals were calibrated internally by the protio impurity of the D_2O solvent (δ 4.63). ^{31}P NMR spectra were obtained by a Bruker Avance 161.98 MHz spectrometer. Absorption spectra were measured using a JASCO V-530 UV−vis spectrophotometer. Fluorescence measurements were performed with a Shimadzu RF-5301pc spectrofluorophotometer. (All emission spectra were collected with the excitation and emission slits set at 5 nm.) Solution CD spectra were carried out with a JASCO-815 CD spectropolarimeter in an aqueous HEPES (0.01 M, 7.4 pH) buffer solution. Elemental analyses were performed with a Vario EL III CHNS elemental analyzer. ESI-MS was performed with a Bruker micrOTOF II mass spectrometer.

Synthesis of $[Zn_2(slys)_2Cl_2]$ (1). An aqueous solution of $ZnCl_2$ (0.681 g, 5 mmol) was added to a methanolic solution of salicylaldehyde (0.5 mL, 5 mmol). After 30 min stirring at room temperature, an aqueous solution of L-lysine hydrochloride (0.913 g, 5 mmol) was added dropwise to the reaction mixture, followed by successive slow addition of a portion of an aqueous NaOH solution (0.2 g, 5 mmol). A dilute methanolic solution of Et_3N (0.7 mL, 5 mmol) was then added to the reaction mixture which was maintained at a pH of 7−8; the stirring was continued for a further 12 h. The reaction mixture was then filtered, and the volume of solvent was reduced via rotary evaporator to afford a yellow residue. A light yellow solid was filtered and washed by methanol and was then dried under vacuum. Colorless single crystals suitable for diffraction were obtained from water−methanol (3:1) mixture. Yield: 49%. C, H, N analysis calcd (%) for $C_{28}H_{48}Cl_2N_4O_{11}Zn_2$ (**1**·$2CH_3OH$·$3H_2O$) (M = 818.34 g mol^{-1}): C 41.09, H 5.91, N 6.85; found: C 41.54, H 5.86, N 6.85. FTIR in KBr disk (ν_{max} /cm^{-1}) 3444, 2941, 1637, 1598, 1473, 1448, 1382, 1290. ^{1}H NMR (D_2O: δ 4.63) 1.817−1.284 (m, 2H$_\gamma$), 1.46−1.52 (m, 2H$_\delta$), 1.70−1.77 (m, 2H$_\beta$), 2.77−2.81 (t, $^3J_{H-H}$ = 7.6 Hz, 2H$_\epsilon$), 3.74−3.76 (t, $^3J_{H-H}$ = 5.7 Hz, 1H$_\alpha$), 6.59−6.66 (m, 2H$_{11,13}$), 7.14−7.22 (m, 2H$_{10,12}$), 8.15 (s, 1H$_{imine}$). ^{13}C NMR (D_2O) 21.17 (C_4), 26.53 (C_5), 34.19 (C_3), 39.10 (C_6), 67.61 (C_2), 115.63 (C_{11}), 119.37 (C_8), 121.53 (C_{13}), 134.51 (C_{10}), 135.84 (C_{12}), 168.07 (C_7), 169.58 (C_9), 180.21 (C_1). MS(ESI) calcd for $C_{26}H_{37}N_4O_8Zn_2$ [**1** − 2Cl$^-$ + 2H_2O − H$^+$]$^+$ 663.03, found 663.0539.

Crystallographic Studies. X-ray diffraction measurements were performed at 293 K with a Bruker SMART 1K CCD diffractometer using graphite-monochromated Mo-Kα radiation (λ = 0.71073 Å). Cell parameters were determined and refined by the SMART program.[7] Data reduction was performed by using SAINT software.[7] The data were corrected for Lorentz and polarization effects. An empirical absorption correction was applied using the SADABS program.[8] All intensity data were corrected for Lorentz and polarization effects. The structures were solved by direct methods using the program SHELXS-97[9] and refined by full matrix least-squares calculations (F^2) by using the SHELXL-97[10] software. All non-H atoms were refined anisotropically against F^2 for all reflections. All hydrogen atoms, except those belonging to the amine nitrogen atom (N2) and the solvent water oxygen atoms, were placed at their calculated positions and refined isotropically. Hydrogen atoms attached to N2 and the water oxygen atoms (O1W,

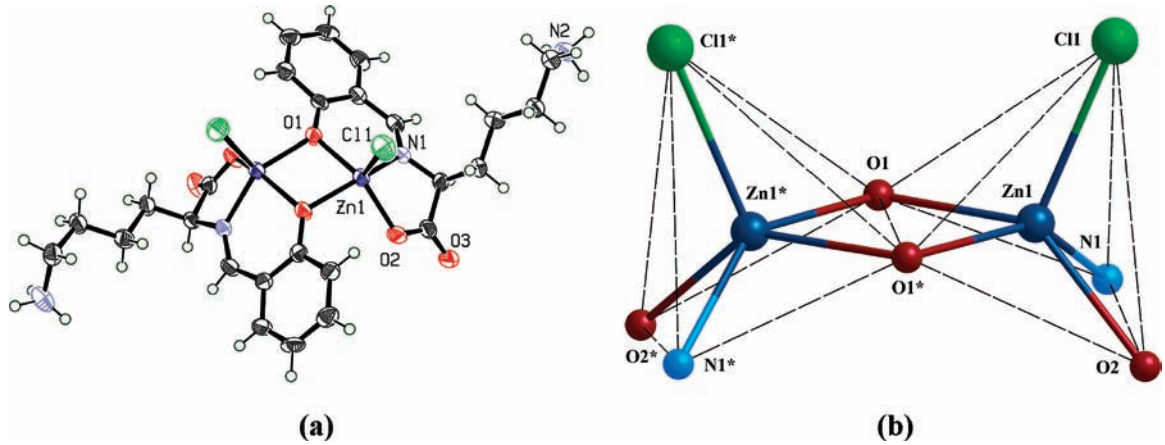

Figure 1. (a) Crystal structure of compound **1**. Thermal ellipsoids at 30% probability level. (b) Core structure of compound **1**. Selected bond lengths [Å]: Zn(1)−N(1), 2.0687(19); Zn(1)−O(1), 2.0753(19); Zn(1)−O(2), 2.0902(19); Zn(1)−Cl(1), 2.2815(18).

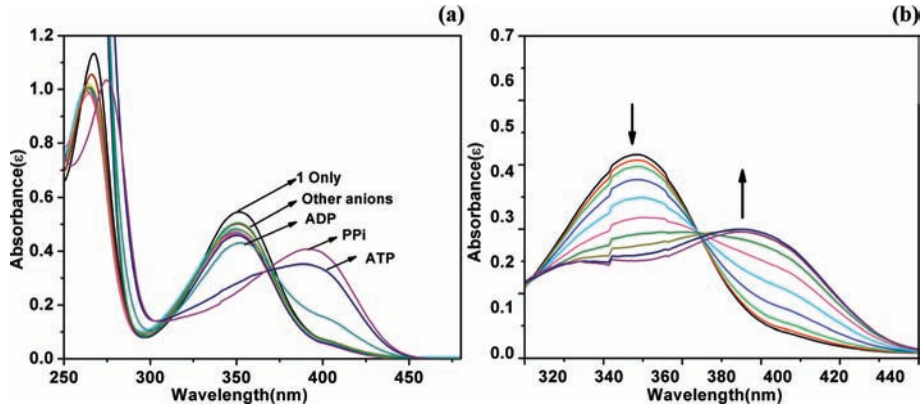

Figure 2. (a) UV−vis spectra of compound **1** (50 μM) with different anions (150 μM). (b) Absorbance titration of **1** (50 μM) in aqueous buffer solution (pH 7.4, 0.01 M HEPES) with increasing amounts of PPi solution (150 μM).

Scheme 1

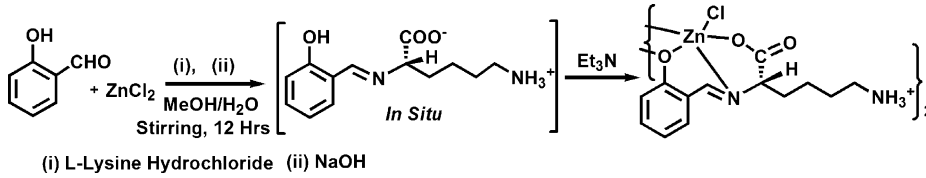

O2W), were located in the difference Fourier maps and refined with isotropic displacement coefficients. Crystal data for the compound **1** is given in Table 1. Selected bond lengths and angles are listed in Table 2. The *.cif file was deposited with the Cambridge Crystallographic Data Centre and the following code was allocated: CCDC-698240. These data can be obtained free of charge via the Internet: www.ccdc.cam.ac.uk/data_request/cif.

Results and Discussion

Synthesis. Compound **1** was synthesized by a typical "one pot" reaction procedure as illustrated in Scheme 1 and was isolated in high yield. This strategic "one pot" synthesis is very effective in such cases where a rational stepwise ligand synthesis is difficult, labor intensive, and/or low yielding.[11]

Compound **1** has been characterized by various spectroscopic techniques and by single crystal X-ray diffraction (vide infra).

Crystal Structure. Compound **1** was found to crystallize in the chiral monoclinic space group *C*2. Its structure reveals that both zinc centers adopt a distorted square pyramidal geometry through tridentate coordination of the *slys* ligand (Figure 1), together with the bridging phenolate oxygens and

(5) (a) Lee, D. H.; Kim, S. Y.; Hong, J.-I. *Angew. Chem., Int. Ed.* **2004**, *43*, 4777. (b) Lee, D. H.; Im, J. H.; Son, S. U.; Chung, Y. K.; Hong, J.-I. *J. Am. Chem. Soc.* **2003**, *125*, 7752. (c) Lee, H. N.; Xu, Z.; Kim, S. K.; Swamy, K. M. K.; Kim, Y.; Kim, S.-J.; Yoon, J. *J. Am. Chem. Soc.* **2007**, *129*, 3828. (d) Lee, J. H.; Park, J.; Lah, M. S.; Chin, J.; Hong, J.-I. *Org. Lett.* **2007**, 3729.

(6) Sensors with amino acid moieties have advantages in terms of subsequent conjugation with peptides and other related biomolecules. See: Jiang, H.; O'Neil, E. J.; DiVittorio, K. M.; Smith, B. D. *Org. Lett.* **2005**, *7*, 3013.

(7) *SMART and SAINT, Area Detector Software Package and SAX Area Detector Integration Program*; Bruker Analytical X-ray: Madison, WI, 1997.

(8) *SADABS, Area Detector Absorption Correction Program*; Bruker Analytical X-ray: Madison, WI, 1997.

(9) Sheldrick, G. M. *Acta Crystallogr.* **1990**, *A46*, 467–473; SHELXS-97 Program for Crystal Structure Determination.

(10) Sheldrick, G. M. *SHELXL-97*; Universität Göttingen: Göttingen, Germany, 1999.

(11) (a) Koner, S.; Saha, S.; Mallah, T.; Okamoto, K.-I. *Inorg. Chem.* **2004**, *43*, 840. (b) Yong, G.-P.; Qiao, S.; Wang, Z.-Y. *Cryst. Growth Des.* **2008**, *8*, 1465.

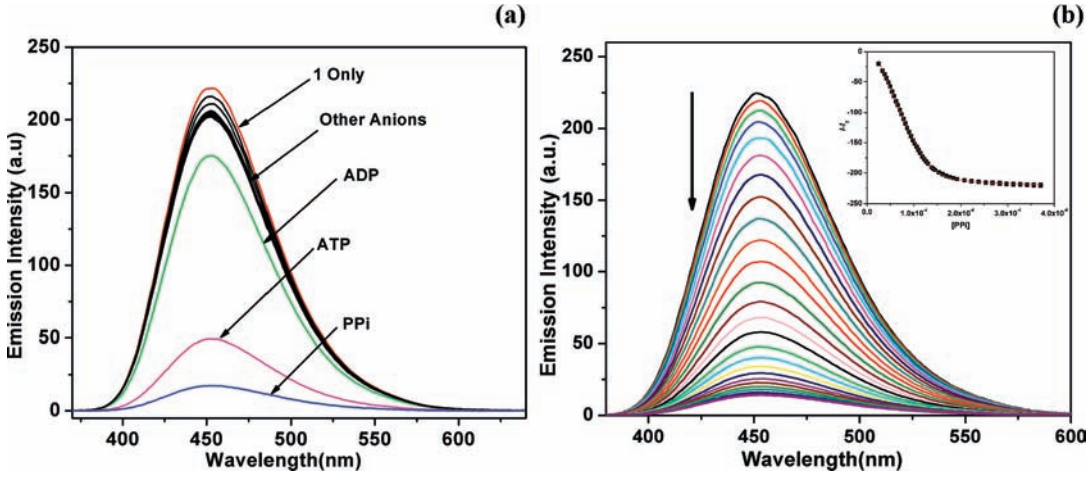

Figure 3. (a) Emission spectra of **1** (50 μM) with different anions (150 μM). (b) Emission titration of **1** (50 μM) in aqueous buffer solution (pH 7.4, 0.01 M HEPES) with increasing amounts of PPi solution (150 μM). (inset) Curve fitting of emission intensity change vs [PPi] at 453 nm. $K_a = 4.06 \times 10^5$ M^{-1} (error ca. 9.8%).

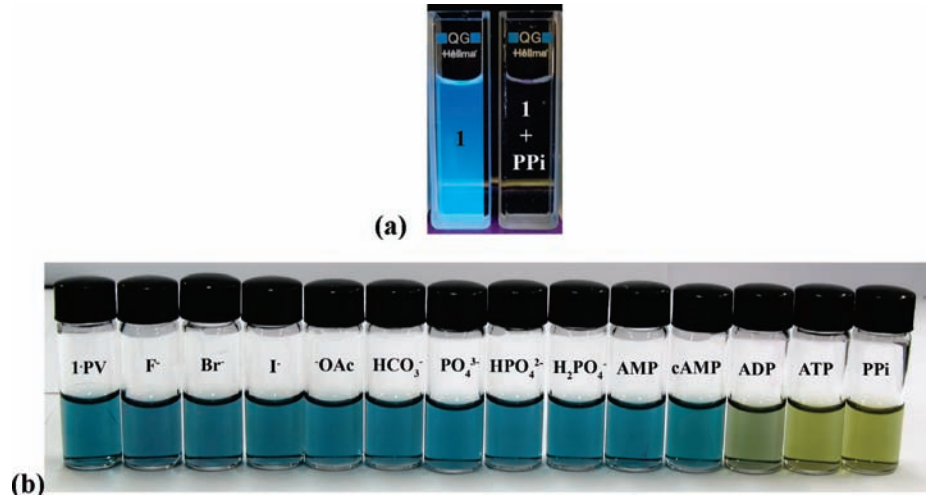

Figure 4. (a) Sensor **1** alone and **1**·PPi (1:4) under UV lamp (365 nm). (b) Color change of the ensemble (50 μM) in the absence and presence of anion (100 μM).

the axial chlorides. The possibility of the displacement of both Cl^- ions that are borne on adjacent metal centers with a multidentate anion attracted us to explore the potential of **1** as a biological phosphate sensing probe.

Electronic Spectroscopy. The UV−vis spectrum of compound **1** in aqueous buffer solution (0.01 M, pH 7.4, HEPES) exhibited two sharp bands at 264 and 352 nm. The band at 352 nm may be assigned to the intraligand charge transfer transition. Since compound **1** absorbs strongly at 264 and 352 nm, the optical effect of the presence of different anions (present as Na^+ salts) was examined in a buffered aqueous titrant (0.01 M, pH 7.4, HEPES) at 25 °C. The addition of PPi caused a decrease in the peak at 352 nm along with the growth of a new peak at 392 nm (Figure 2). The ~40 nm bathochromic shift indicates sensor-PPi binding. However, upon addition of the structurally related species ATP and ADP, smaller shifts (36 and 1 nm, respectively) were observed. No significant changes were observed for other anions such as F^-, Br^-, I^-, AcO^-, HCO_3^-, $H_2PO_4^-$, HPO_4^{2-}, PO_4^{3-}, adenosine monophosphate (AMP), and cyclic adenosine monophosphate (cAMP). Binding stoichiometry was determined via indicator displacement assays (vide infra). Job plots were prepared from the UV−vis titration data and in all cases confirmed 1:1 binding of **1** and the respective phosphate (PPi, ATP, or ADP) (Supporting Information, Figure S18).

Emission Spectroscopy. Compound **1** is highly fluorescent, in both the solution phase and as a solid. Under neutral aqueous conditions (0.01 M HEPES buffer, pH 7.4), compound **1** exhibits intense blue fluorescence ($\lambda_{ex} = 352$ nm, $\lambda_{em} = 453$ nm, $\Phi_F = 0.17$).[12] The fluorescence of **1** is generated from the 2-hydroxybenzylidene amino group in which C=N isomerization is inhibited because of Zn^{2+} complexation.[13] After addition of 3 and 8 equiv of PPi, the fluorescence intensity decreased ~13-fold, and ~47-fold ($\Phi_F = 0.003$), respectively (Figures 3b and 4a). It is expected that PPi binding weakens the Zn−N and $Zn-O_{(phenolic)}$ bonds, and acts to reinstate C=N isomerization, thus allowing for fluorescence quenching. Hong et al. reported similar $Zn-O_{(phenolic)}$ bond weakening during PPi chelation.[5a] Ha-

(12) Quantum yields were calculated using fluorescein as a reference.
(13) (a) Ray, D.; Bharadwaj, P. K. *Inorg. Chem.* **2008**, *47*, 2252. (b) Wu, J.-S.; Liu, W.-M.; Zhuang, X.-Q.; Wang, F.; Wang, P.-F.; Tao, S.-L.; Zhang, X.-H.; Wu, S.-K.; Lee, S.-T. *Org. Lett.* **2007**, *9*, 33.

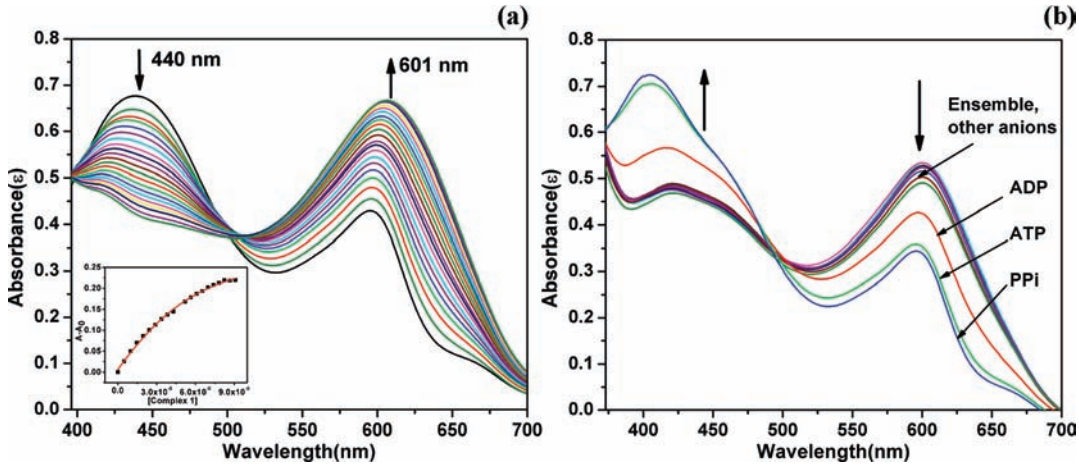

Figure 5. (a) UV−vis spectrum obtained by addition of solution of **1** to an aqueous buffer solution containing PV (50 μM) (10 mM HEPES, pH 7.4). (inset) Curve fitting of absorbance change vs [Complex **1**] at 601 nm, $K_a = 4.99 \times 10^4$ M^{-1} (error *ca.* 18%) (b) UV−vis spectrum obtained by addition of different anion solution (100 μM) to an aqueous buffer [**1**·PV] 1:1 ensemble (50 μM) [10 mM HEPES, pH 7.4].

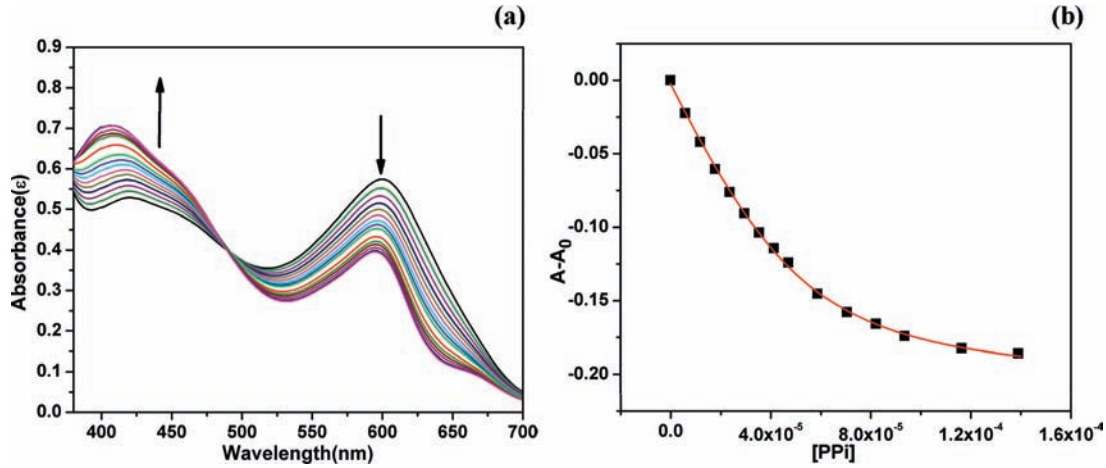

Figure 6. UV−vis titration spectrum obtained by addition of PPi solution (0−150 μM) to an aqueous buffer solution containing the [**1**·PV] 1:1 ensemble (50 μM) [10 mM HEPES, pH 7.4]. (b) Curve fitting of absorbance change vs [PPi] at 601 nm. $K_a = 8.79 \times 10^4$ M^{-1} (error ca. 7.5%).

machi et al. observed coordinative bond disruption between a xanthene C−O oxygen and two zinc centers. But in this report, the fluorescence is turned *on* because of the recovery of the conjugated xanthene moiety.[3k] The apparent equilibrium constant of association (K_a) was determined by fluorescence to be $4.06 \pm 0.4 \times 10^5$ M^{-1} for **1**·PPi.[14] Comparatively small fluorescence quenching was observed for ATP (4.5-fold) and ADP (1.3-fold) after addition of 3 equiv of each analyte. The fluorescence intensity decreased ~18-fold after the addition of 8 equiv of ATP and ~8.5-fold after addition of 40 equiv of ADP. The apparent K_a was also found to be small. This value was measured to be $(3.36 \pm 0.2) \times 10^5$ M^{-1} for **1**·ATP and $(9.14 \pm 0.06) \times 10^3$ M^{-1} for **1**·ADP. Thus, the binding tendency was established to be as follows: PPi ≥ ATP > ADP. The greater interaction that PPi and ATP have with the zinc complex is due to the greater electronic charge density on these phosphate groups than that for ADP. But, the binding interaction of PPi is slightly greater than for ATP, possibly because of a steric interaction involving the adenosine group of ATP with the lysine group of the dizinc complex.

Colorimetric Sensing. Naked eye colorimetric detection of biologically important anions by indicator displacement assays (IDAs), or a chemosensing ensemble (CE) approach, is popular and well accepted.[15] In this light, we utilized the pyrocatechol violet (PV) chromogenic indicator because it is known to bind to species containing two adjacent metal centers.[3a5e] In our case, during the titration of **1** to a PV solution, the intense absorption at 440 nm gradually decreased while a band at 601 nm concomitantly increased. Reversibility was demonstrated when 2 equiv each of PPi, ATP, and ADP were added and the yellow color of PV was restored (Figure 4b, 5). Other anions including biologicaly important monophosphate anions did not allow for color recovery even when more than 10 equiv were added, suggesting the greater affinities of PPi, ATP, and ADP over

(14) (a) Connors, K. A. *Binding Constants*; Wiley: New York, 1987. (b) Valeur, B.; Pouget, J.; Bourson, J.; Kaschke, M.; Ernsting, N. P. *J. Phys, Chem.* **1992**, *96*, 6545.

(15) (a) Niikura, K.; Metzger, A.; Anslyn, E. V. *J. Am. Chem. Soc.* **1998**, *120*, 8533. (b) Metzger, A.; Anslyn, E. V. *Angew. Chem., Int. Ed.* **1998**, *37*, 649. (c) Wiskur, S. L.; Haddou, H. A.; Lavigne, J. J.; Anslyn, E. V. *Acc. Chem. Res.* **2001**, *34*, 963. (d) Nguyen, B. T.; Anslyn, E. V. *Coord. Chem. Rev.* **2006**, *250*, 3118. (e) Fabbrizzi, L.; Licchelli, M.; Taglietti, A. *Dalton Trans.* **2003**, 3471.

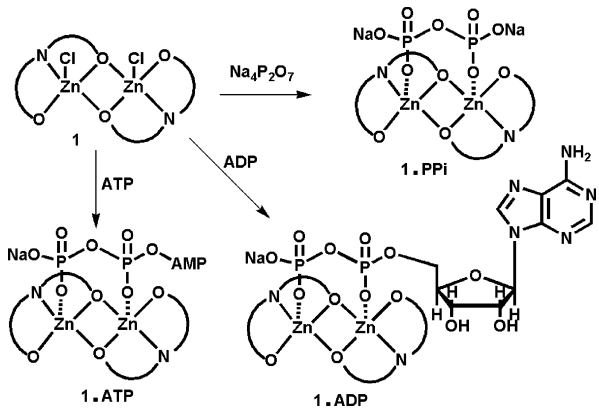

Figure 7. Proposed binding modes of phosphate ions with compound **1**.

Table 3. Association Constant (K_a) Values Calculated from Emission Titration and Indicator Displacement Methods in Aqueous Buffer Solution (pH = 7.4) at 25 °C

	association constant (K_a)	
anions	emission titration (λ_{em} at 453 nm)	IDA (λ_{max} at 601 nm)
PPi	4.06×10^5 M^{-1} (error ca. 9.8%)	8.79×10^4 M^{-1} (error ca. 7.5%)
ATP	3.36×10^5 M^{-1} (error ca. 5.9%)	8.77×10^4 M^{-1} (error ca. 9%)
ADP	9.14×10^3 M^{-1} (error ca. 3%)	1.40×10^4 M^{-1} (error ca. 26%)
1·PV		4.99×10^4 M^{-1} (error ca. 18%)

other anions for the dizinc receptor (Figure 5). The Job plot analyses confirmed the predicted 1:1 stoichiometry of binding of **1** to PV (Supporting Information, Figure S18). The association constant, K_a of **1**·PV was determined to be $4.99 \pm 0.9 \times 10^4$ M^{-1}. During titration of 1:1 (**1**·PV) ensemble (50 μM) with increasing amount of PPi (150 μM), the band at 440 nm gradually increased in intensity while the band at 601 nm gradually decreased (Figure 6). The K_a's of PPi/ATP/ADP were also determined using **1** and titrating the aqueous chemosensing ensemble solution (pH 7.4) containing **1** and PV with these anions, giving a similar trend: PPi ≥ ATP > ADP (Table 3). Though the K_a of **1**·ADP is somewhat smaller than that for **1**·PV, a relatively high concentration of ADP is able to replace PV from the **1**·PV ensemble. Both the fluorometric and colorimetric titration results suggest that compound **1** is a highly selective sensor for polyphosphate species.

Possible Phosphate Binding Modes and Evidence of Binding from ^{31}P NMR and Circular Dichroism (CD) Spectroscopy. It is clear that when PPi, ATP, or ADP is added, two Zn−Cl bonds must dissociate to allow for two Zn−O bonds. While we cannot confirm front- or rear-side nucleophilic attack, the possible phosphate binding modes with compound **1** are illustrated in Figure 7. Substantiation of this behavior comes from ^{31}P NMR and circular dichroism (CD) spectroscopy. First, phosphate-sensor interactions are supported by ^{31}P NMR spectroscopy. The addition of 1 equiv of **1** to a solution of $Na_4P_2O_7$ in D_2O resulted in a shifting of the pyrophosphate ^{31}P signal from −6.03 to −4.43 ppm (Figure 8). This large shift is also observed for ATP and ADP under analogous conditions. In the case of ATP, the triplet and doublet signal for the β- and γ-P atoms are shifted by 3.98 and 5.28 ppm, respectively; the shift for the α-P-atom is relatively small (0.62 ppm) strongly suggesting that

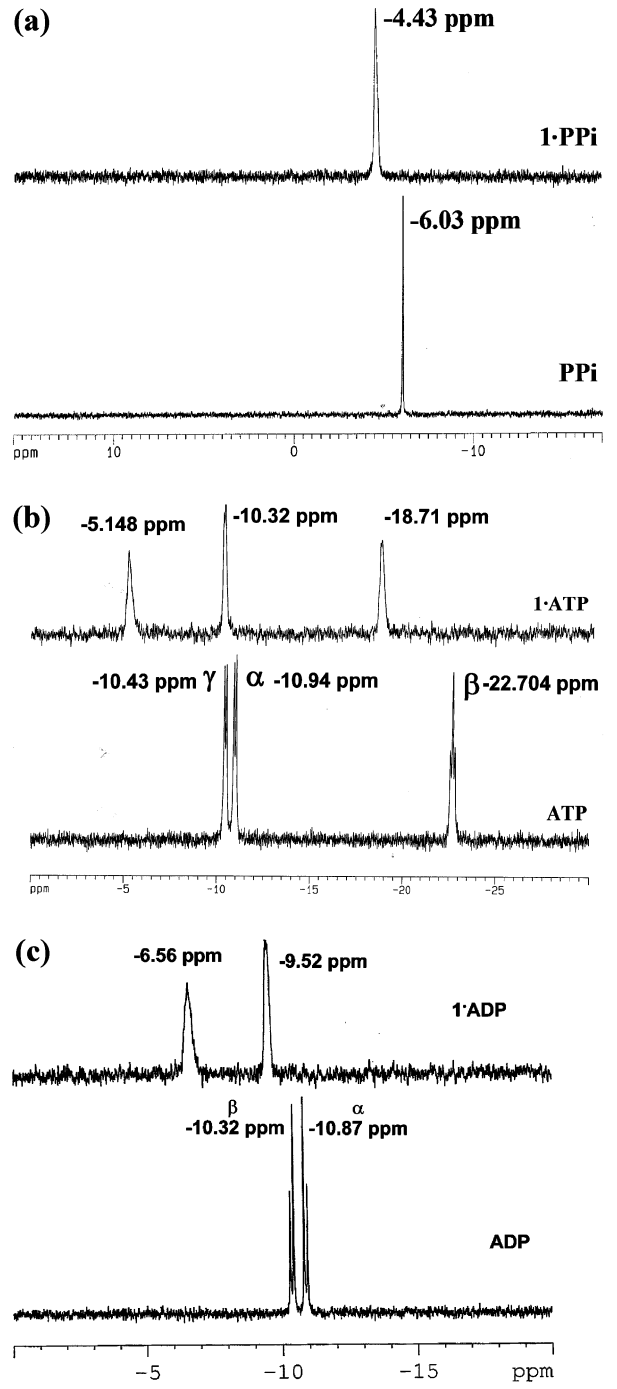

Figure 8. ^{31}P NMR spectra. (a) PPi with compound **1** (1:1) in D_2O, (b) ATP with **1** (1:1) in D_2O, and (c) ADP with **1** (1:1) in D_2O.

the α-P center is not interacting with the zinc centers. ^{31}P NMR spectral data again supports the lesser binding affinity of ADP over that of ATP, as the chemical shift change of the α-P atom ADP is smaller (1.45 ppm) than that for the β-P-atom of ATP.[7b] This change may be due to the greater negative charge density on ATP.[3k,16]

Another advantage of our sensor is that it is chiral because of the presence of L-lysine residues. Thus, phosphate binding is also investigated by solution CD spectroscopy. In the

(16) (a) Ojida, A.; Park, S.-K.; Oka, Y. M.; Hamachi, I. *Tetrahedron Lett.* **2002**, *43*, 6193. (b) Jose, D. A.; Mishra, S.; Ghosh, A.; Shrivastav, A.; Mishra, S. K.; Das, A. *Org. Lett.* **2007**, *9*, 1979.

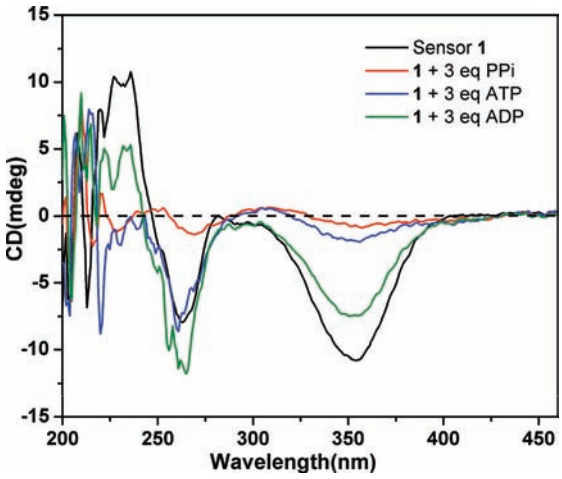

Figure 9. Circular Dichroism (CD) spectra of compound **1** and with 3 equiv of ADP, ATP, and PPi in aqueous buffer solution (pH 7.4, 0.01 M HEPES, cell path length = 1 cm).

absence of phosphate ions, the sensor shows a negative Cotton effect at 352 nm. In the presence of ADP, the intensity is only slightly decreased. For ATP and PPi, large decreases in CD intensity are observed which implies that some conformational change occurs in the system upon anion binding (Figure 9).

Selectivity and Sensitivity. Since phosphate ion binding and detection occurs through Cl^- loss, we conducted displacement studies. When we titrated a 1:4 sensor/PPi mixture with excess Cl^- ions, the fluorescence was not restored, suggesting greater affinity of PPi than Cl^- for the zinc centers (Supporting Information, Figure S15). Sensor **1** detects small amounts of PPi (4 equiv) by effective quenching of the fluorescence in the presence of 50 equiv of monophosphates (Supporting Information, Figure S15). Finally we determined that the working pH range of **1** for phosphate ion sensing is from 6.8 to 9.5, but its stability and sensitivity are both better at pH 7.4 (see Supporting Information, Figure S19).

Conclusion

In conclusion, we have prepared a chiral fluorescent zinc complex for the fluorometric and colorimetric (IDA) sensing of PPi, ATP, and ADP in water at physiological pH. This synthesis involves an easy "one pot" method wherein the lysine-based Schiff base ligand portion is generated in situ. Owing to the fluorescent properties of this complex (Φ_F = 0.17), the compound and its changes can be conveniently characterized via UV−vis spectroscopy but also in detail by NMR spectroscopic techniques and ultimately by single-crystal X-ray diffraction. The dizinc complex was tested with a variety of halides, carbonate, acetate, and common phosphate based anions, as well as a variety of biologically relevant phosphate anions in water at physiological pH. The compound was found to act as a highly selective fluorescent ON-OFF sensor for PPi. Fluorometric and colorimetric (indicator displacement assays) titration results suggest that compound **1** is selective for phosphate ions in this manner: PPi ≥ ATP > ADP. The pendant $-NH_2$ groups can allow for facile attachment to peptide moieties or nanoparticle surfaces. Work in this direction has been initiated in this laboratory.

Acknowledgment. D.G.C. acknowledges support from KOSEF (Grant R01-2008-000-12388-0). S.K. is grateful to the Ministry of Education, Science & Technology for a BK 21 postdoctoral fellowship. Hack Soo Shin is gratefully acknowledged for his help in acquiring NMR data. We thank S. J. Hong of Kangwon National University for technical assistance.

Supporting Information Available: All types of NMR spectra related to this work, UV−vis, and emission spectra, in PDF and CIF format. This material is available free of charge via the Internet at http://pubs.acs.org.

IC8022387